

# Interchromosomal associations between alternatively expressed loci

Charalampos G. Spilianakis<sup>1</sup>, Maria D. Lalioti<sup>2\*</sup>, Terrence Town<sup>1\*</sup>, Gap Ryol Lee<sup>1</sup> & Richard A. Flavell<sup>1,3</sup>

The T-helper-cell 1 and 2 (T<sub>H</sub>1 and T<sub>H</sub>2) pathways, defined by cytokines interferon- $\gamma$  (IFN- $\gamma$ ) and interleukin-4 (IL-4), respectively, comprise two alternative CD4<sup>+</sup> T-cell fates, with functional consequences for the host immune system. These cytokine genes are encoded on different chromosomes. The recently described T<sub>H</sub>2 locus control region (LCR) coordinately regulates the T<sub>H</sub>2 cytokine genes by participating in a complex between the LCR and promoters of the cytokine genes *Il4*, *Il5* and *Il13*. Although they are spread over 120 kilobases, these elements are closely juxtaposed in the nucleus in a poised chromatin conformation. In addition to these intrachromosomal interactions, we now describe interchromosomal interactions between the promoter region of the IFN- $\gamma$  gene on chromosome 10 and the regulatory regions of the T<sub>H</sub>2 cytokine locus on chromosome 11. DNase I hypersensitive sites that comprise the T<sub>H</sub>2 LCR developmentally regulate these interchromosomal interactions. Furthermore, there seems to be a cell-type-specific dynamic interaction between interacting chromatin partners whereby interchromosomal interactions are apparently lost in favour of intrachromosomal ones upon gene activation. Thus, we provide an example of eukaryotic genes located on separate chromosomes associating physically in the nucleus via interactions that may have a function in coordinating gene expression.

The subnuclear localization of chromatin is not random, and specific genetic loci or whole chromosomes reside in specific locations within the nucleus<sup>1</sup>, where each chromosome is localized in a limited and specific space, called a 'territory', and DNA sequences within a chromosome are organized into euchromatin or heterochromatin. In some cases, large chromosomal loops containing active genes extend outside of the defined chromosomal territories<sup>2</sup>. As cellular differentiation proceeds, changes in transcriptional activity are often coupled with changes in subnuclear localization of chromosomes. Silent genes in developing B and T cells are repositioned in the nucleus at pericentromeric heterochromatin<sup>3–5</sup>. Transcriptional regulatory elements such as locus control regions, enhancers or insulators act by repositioning specific genetic loci to regions with active or silent transcription<sup>6</sup>. Furthermore, sequence-specific DNA-binding proteins may confer their action by directly repositioning these loci to relevant chromatin compartments<sup>7–12</sup>.

It has been proposed that transcription and RNA-processing events occur in the space between the chromosome territories in an area called the interchromosome domain compartment<sup>1</sup>. The higher order of chromatin organization and its links with transcription have been extensively studied at different levels, such as the chromosomal territories or large-scale structures greater in size than the 30-nm chromatin fibre<sup>13,14</sup>. Although all studies so far have focused on the inter-relationship between transcriptional activation and subnuclear localization, there has been no evidence for direct physical interaction between inter-related genetic loci localized on different chromosomes. The recently developed chromosome conformation capture technique (3C)<sup>15–18</sup> provides a powerful tool to study interchromosomal interactions with high accuracy in molecular terms.

We recently described large-scale intrachromosomal interactions during the differentiation of naive CD4<sup>+</sup> T cells to T<sub>H</sub>1 or T<sub>H</sub>2 cells.

In direct correlation with the expression profiles of the T<sub>H</sub>2 cytokines, several DNase I hypersensitive sites have been characterized for the T<sub>H</sub>2 cytokine gene locus on mouse chromosome 11 (refs 19–25). Similarly, the expression of the IFN- $\gamma$  gene (*Ifng*) located on mouse chromosome 10 is regulated by two conserved regions: *Ifng* CNS1 located 5 kilobases (kb) upstream and *Ifng* CNS2 located 18 kb downstream of the initiation codon of the murine *Ifng* gene<sup>25,26</sup>. We now report that the *Ifng* gene located on mouse chromosome 10 physically interacts with the *Il5* cytokine promoter, *Rad50* promoter and RHS6 DNase I hypersensitive site of the T<sub>H</sub>2 LCR, all located in the T<sub>H</sub>2 cytokine gene locus on mouse chromosome 11. The interactions are extremely strong in naive CD4<sup>+</sup> T cells and are subsequently greatly reduced after the differentiation of naive T cells to effector T<sub>H</sub>1 or T<sub>H</sub>2 cells. In contrast, non-T-cell types do not exhibit these interactions. Concomitant with the loss of these interchromosomal interactions, in T<sub>H</sub>1 cells the *Ifng* gene region instead strengthens intrachromosomal interactions with the *Ifng* CNS2 region located downstream of the *Ifng* gene.

We suggest that there are dynamic intra- and interchromosomal interactions between specific genetic loci that regulate transcriptional initiation or silencing of these loci. We also suggest that one of the functions of LCRs in addition to regulating the expression of adjacent genes is to participate in developmentally regulated interchromosomal interaction of related genes. It is likely that interchromosomal association of genes that are coordinately regulated will be a common feature of gene organization in the nucleus of most higher organisms.

**Interchromosomal interactions between *Ifng* and T<sub>H</sub>2 loci.** In cells of the T-cell lineage and other cell types we have recently reported that specific intrachromosomal interactions occur in the T<sub>H</sub>2 cytokine gene locus containing the cytokine genes *Il4*, *Il5* and *Il13*. The promoters of the cytokine genes are located in close proximity to the

<sup>1</sup>Section of Immunobiology, and <sup>2</sup>Department of Genetics, Yale University School of Medicine, New Haven, Connecticut 06520, USA. <sup>3</sup>The Howard Hughes Medical Institute, New Haven, Connecticut 06520, USA.

\*These authors contributed equally to this work.

$T_H2$  LCR in the nucleus of certain cell types, probably functioning to facilitate coordinated transcriptional regulation of cytokine-encoding genes<sup>18</sup>. In an attempt to unravel the regulatory effects of the  $T_H2$  LCR in other genes, we used the 3C technique to identify whether there are any physical interchromosomal interactions of the  $T_H2$  locus with the murine *Ifng* locus, the signature cytokine of the alternative  $T_H1$  cell lineage. The organization of the loci and the fragments we used in the 3C analysis are depicted in Fig. 1a–e. As a control locus for the 3C analysis, we used the murine *Gm-csf* gene (also called *Csf2*), which is expressed non-selectively in both  $T_H1$  and  $T_H2$  cells, and is located on the same mouse chromosome (chromosome 11) as the  $T_H2$  locus, about 620 kb upstream of the *Il4* gene. We used the equations in Fig. 1f, g in order to obtain the crosslinking frequency between two fragments. As described previously<sup>16,18</sup>, we corrected the values of the polymerase chain

reaction (PCR) signals we obtained for a given cell type with those obtained for adjacent fragments of the *Gapd* or the  $\beta$ -globin locus, to control for chance interactions (see Supplementary Methods). Clearly, these are highly conservative background controls to choose, because the physical distance between these control fragments is so small as to render them in complete linkage disequilibrium, whereas for DNA segments located on different chromosomes, random association of fragments would occur much less frequently. Thus, we probably underestimate interchromosomal interactions.

We performed the 3C analysis for the *Ifng* locus and the  $T_H2$  cytokine gene locus. Surprisingly, strong and specific interactions were detected between the *Ifng* gene and three fragments of the  $T_H2$  cytokine locus, covering the constitutive DNase I hypersensitive site RHS6 of the  $T_H2$  LCR (fragment H), the *Rad50* promoter (fragment

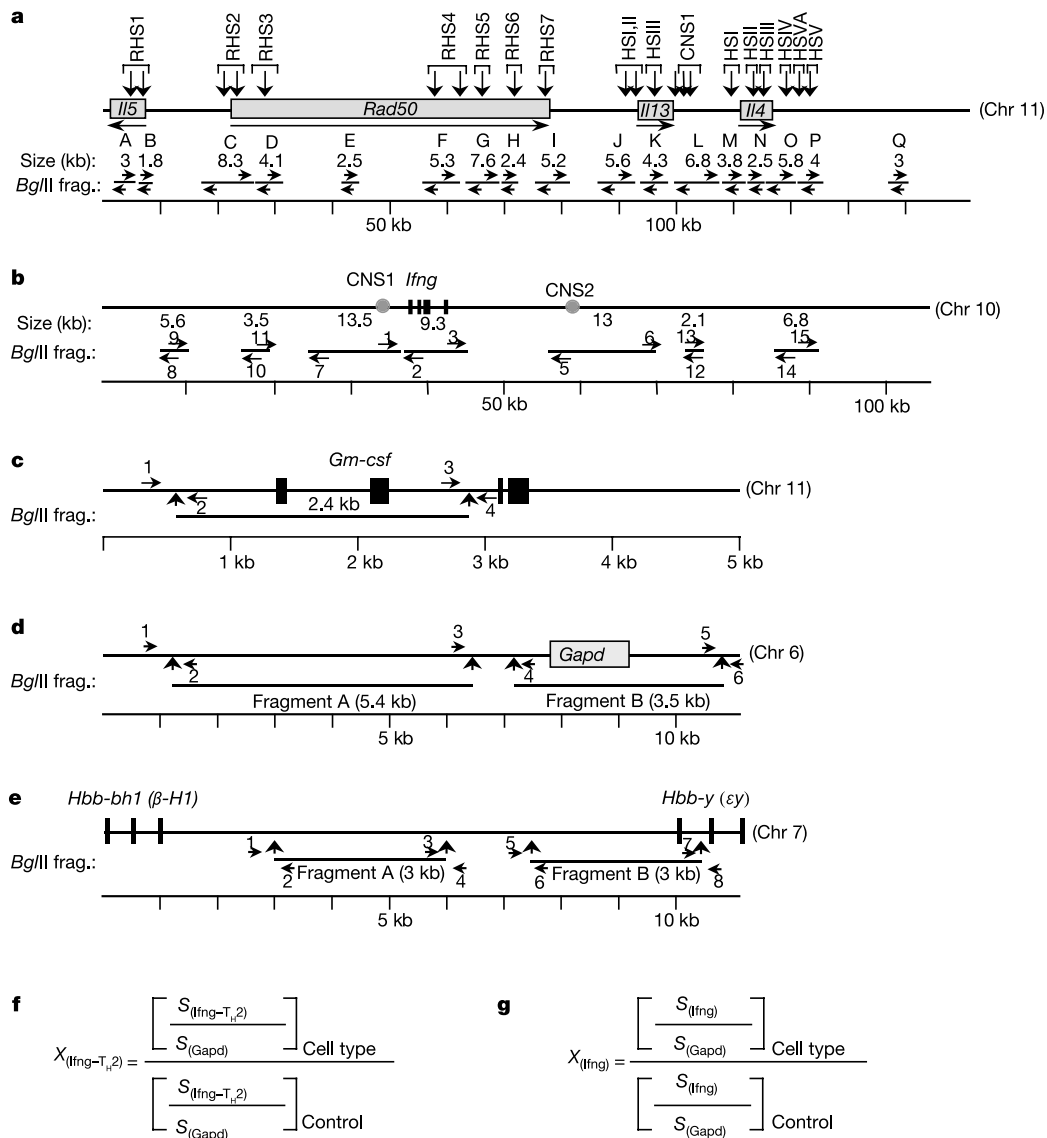


**Figure 1 | Spatial organization of the genetic loci used for the 3C analysis.**

**a**, Schematic representation of the murine  $T_H2$  cytokine locus on mouse chromosome 11. Arrows on the top represent all the DNase I hypersensitive sites characterized so far. Below the locus are presented all the *Bgl*III restriction enzyme fragments used in our 3C analysis and their relative position on the locus. **b–e**, Schematic representation of the murine *Ifng* locus (**b**), *Gm-csf* locus (**c**), *Gapd* locus (**d**) and  $\beta$ -globin locus (partial) (**e**). **f**, The equation used for the interchromosomal interactions in the 3C analysis.  $X$  is the relative crosslinking frequency between two fragments.

**g**, The equation used for the *Ifng* intrachromosomal interactions in the 3C analysis. For the *Gapd* control the values we obtained by dividing the PCR signal ( $S$ ) detected in a cell tissue with the PCR signal for its control template were 0.45 (naive T cells), 0.63 ( $T_H1$ ) and 0.72 ( $T_H2$ ). The values we obtained using the  $\beta$ -globin locus as a control were accordingly 0.46, 0.64 and 0.69, which are comparable to those for the *Gapd* gene. Re-analysing the data using  $\beta$ -globin as a control does not change the interpretation of the results.

C) and *Il5* promoter (fragment B), respectively (Fig. 2a–c). The DNase I hypersensitive site RHS6 of the  $T_H2$  LCR is the only one present in naive T cells,  $T_H1$  and  $T_H2$  cells<sup>24</sup>; *Rad50* promoter DNase I hypersensitive sites are also constitutively hypersensitive. Notably, in naive T cells the interactions were very strong, with a crosslinking frequency of 4–5, a value similar to that found for the strongest intrachromosomal interactions in the *Il4* locus<sup>18</sup>. Upon differentiation of naive T cells to effector  $T_H1$  and  $T_H2$  cells the crosslinking frequencies became much lower. Using the 3C analysis we also determined the interaction of *Ifng* CNS1 and *Ifng* CNS2 fragments with all fragments in the  $T_H2$  locus, but no specific interaction was detected (Fig. 2d). All of the above-mentioned results were highly reproducible over six experiments.

**Interchromosomal interactions require RHS7.** To determine whether the  $T_H2$  LCR is required for the interchromosomal interactions, a specific region covering DNase I hypersensitive site RHS7 of the LCR was deleted; this region seems to be the most important element of the LCR and is essential for  $T_H2$  cytokine gene expression. Furthermore, in previous studies we found that RHS7 deletion leads to the abrogation of all RHS6 interactions with other *cis*-elements on the *Il4* locus<sup>27</sup>. Therefore we hypothesized that RHS7 deletion would cause loss of RHS6 interactions with the *Ifng* locus. We prepared templates for the 3C analysis and measured the relative crosslinking frequency between the *Ifng* gene and any fragment in the  $T_H2$  cytokine locus. RHS7 was required for the interchromosomal interaction of the *Ifng* gene fragment with the  $T_H2$  locus. Notably, in naive T cells and to a lesser extent in effector  $T_H1$  and  $T_H2$  cells, the interactions of the *Ifng* gene with the *Il5* promoter, *Rad50* promoter and RHS6 were greatly reduced, from a crosslinking frequency of about 5 to a crosslinking frequency with a value close to 1, the same

value considered to be background in an intrachromosomal interaction (Fig. 2a–c).

To make sure that the results for the interchromosomal interaction of different loci were not an artefact of the 3C technique, we performed experiments analysing the crosslinking frequency between different fragments from several genetic loci in different chromosomes. No interactions were detected by the 3C analysis for restriction fragments A and B of the *Gapd* locus with any fragment in the  $T_H2$  locus. Similarly, interactions were not detected between the seven restriction fragments of the *Ifng* locus and the two restriction fragments in the *Gapd* locus, between the *Ifng* locus and the *Gm-csf* locus, nor between the *Gapd* locus and the *Gm-csf* locus (Fig. 2d).

**Inter- to Intrachromosomal interaction switch in effector T cells.** Because we found that the interaction between the *Ifng* gene and the specific regions of the  $T_H2$  locus are largely lost during the differentiation of naive T cells to effector T-helper cells, we wanted to see whether new compensating interactions emerge in effector cells that might replace the interchromosomal interactions described. We therefore analysed the intrachromosomal interactions between seven *Bgl*III restriction enzyme fragments in the *Ifng* locus. We found that the restriction enzyme fragment covering the conserved sequence *Ifng* CNS1 upstream of the *Ifng* gene interacted with the *Ifng* gene fragment, as previously described<sup>28</sup>, but not with the fragment spanning *Ifng* CNS2 (Fig. 3a–c). This interaction was profound in naive T cells, with a crosslinking frequency close to 5; in effector  $T_H1$  and  $T_H2$  cells the interaction was present but was weaker compared to that observed in naive T cells. We next analysed the crosslinking frequencies of the *Ifng* gene with the upstream and downstream conserved regions and the control regions, and we found it to interact

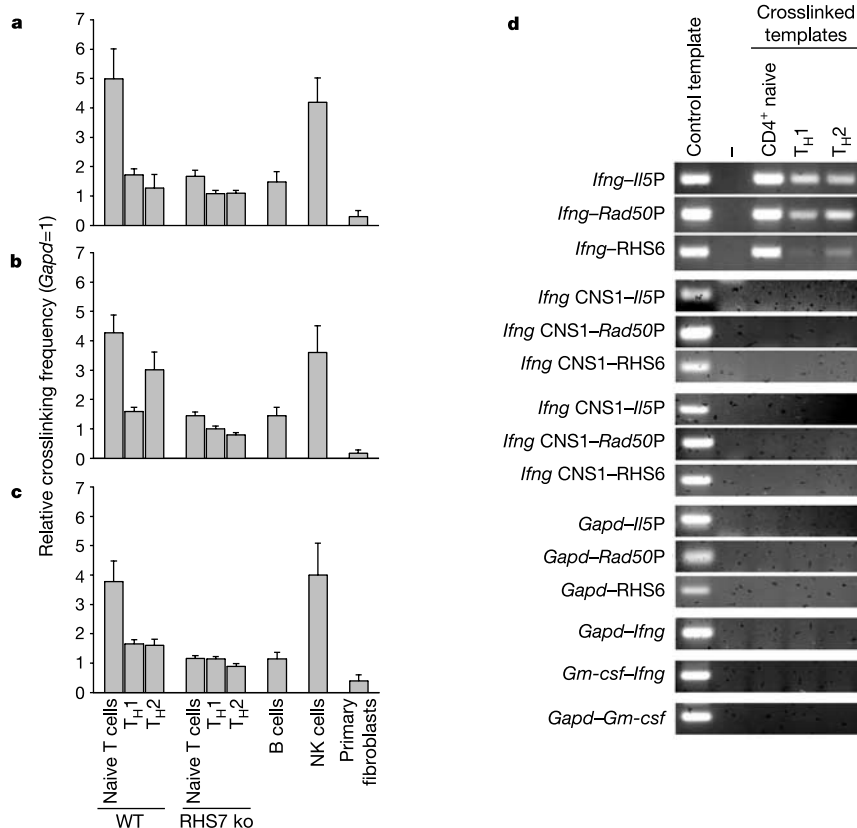


**Figure 2 | Interchromosomal,  $T_H2$  LCR-regulated interactions.** On the y axis the relative crosslinking frequency between two fragments is presented. The value of 1 is the crosslinking frequency for the two closely linked GAPD fragments. **a–c**, Relative crosslinking frequencies for the interchromosomal interaction between the *Ifng* gene and the *Il5* promoter (**a**), the *Rad50*

promoter (**b**) and RHS6 DNase I hypersensitive site of the  $T_H2$  LCR (**c**). Error bars represent the standard deviation between at least three repeats for each of two cell preparations. **d**, PCR signals detected from the 3C analysis for naive T cells,  $T_H1$  and  $T_H2$  cells using pairs of primers for the regions indicated on the left.

with *Ifng* CNS1 in all three cell types (Fig. 3d–f), and to specifically interact with *Ifng* CNS2 in T<sub>H</sub>1 cells (Fig. 3e). The *Ifng* CNS2 fragment was associated with the *Ifng* gene only in T<sub>H</sub>1 cells (Fig. 3h). Although the crosslinking frequency value of  $2.1 \pm 0.35$  detected for the latter interaction is only double that of the value 1, set for the background (based upon *Gapd*–*Gapd* interactions), we consider this significant because this association was only detected in T<sub>H</sub>1 cells and not in naive T cells nor T<sub>H</sub>2 cells, where the interactions were in fact completely undetectable (that is, much lower even than the *Gapd* background). There were no interactions detected between IFN- $\gamma$  CNS1 and IFN- $\gamma$  CNS2.

**Co-localization of the *Ifng* and T<sub>H</sub>2 loci revealed by FISH.** To confirm the interchromosomal interactions between the *Ifng* and T<sub>H</sub>2 loci, fluorescence *in situ* hybridization (FISH) experiments were performed. Hybridizations were performed using sorted naive CD4<sup>+</sup> T cells or T<sub>H</sub>1 and T<sub>H</sub>2 cells, differentiated for 5 days, from wild-type or RHS7<sup>-/-</sup> mice. First, we performed the experiments for wild-type naive T cells, T<sub>H</sub>1 and T<sub>H</sub>2 cells using two-dimensional FISH. These experiments were repeated twice using two independent preparations of wild-type T cells (Supplementary Fig. 1). These FISH data confirmed our results obtained using the 3C technique. In about 50% of wild-type naive T cells one allele of the T<sub>H</sub>2 locus was

co-localized with one allele of the *Ifng* locus, whereas this interaction was considerably decreased in effector T<sub>H</sub>1 and T<sub>H</sub>2 cells. As an important control, we examined the co-localization of the *Gapd* locus (located in chromosome 6) with the T<sub>H</sub>2 locus or the *Ifng* locus. In all cell types the percentage of cells having one allele for the T<sub>H</sub>2 or *Ifng* gene loci co-localized with the *Gapd* locus was always low and is probably the background level of the technique, because it is not confirmed with the 3C method (Supplementary Fig. 1). We wanted to expand further our analysis after these findings; therefore we used a FISH technique where the three dimensional structure of the cells is maintained. We repeated the experiments for the wild-type and RHS7<sup>-/-</sup> cells (Fig. 4a–f). In three independent experiments with two preparations of cells we observed that the percentage of naive CD4<sup>+</sup> T cells having at least one allele of the T<sub>H</sub>2 locus co-localized with one allele of the *Ifng* locus was close to 40%, compared with only 10–13% observed in effector T<sub>H</sub>1 and T<sub>H</sub>2 cells (Fig. 4a, c, e). In RHS7<sup>-/-</sup> naive T cells the percentage of cells with at least one allele co-localized was increased to 71.5%. However, more careful analysis of the cells revealed that in wild-type cells the signals scored as co-localized had a distance of  $\leq 5$  pixels, but in more than 85% of RHS7<sup>-/-</sup> naive T cells that showed co-localization, the distance between the co-localized signals was greater (about 5–8 pixels),

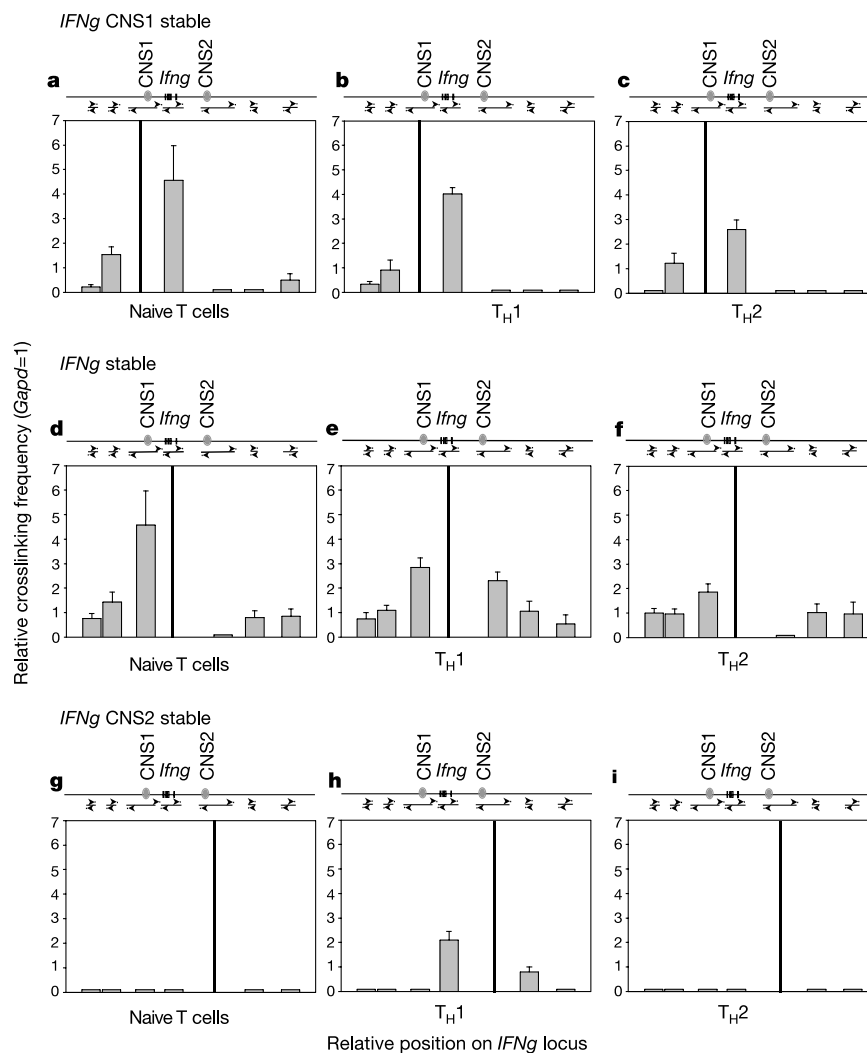


**Figure 3 | Intrachromosomal enhancer-promoter interactions in the *Ifng* gene.** a–i, 3C analysis for the *Ifng* locus (a–c), CNS1 (d–f) and CNS2 (g–i). Error bars represent the standard deviation between four repeats of all PCR reactions. The x axis represents the relative position of fragments on the *Ifng* locus; the y axis represents the relative crosslinking frequency between two

fragments. The value of 1 is the crosslinking frequency for the two closely located GAPD restriction enzyme fragments. ‘Stable’ means that the pair of primers for the designated restriction fragment was combined with the pair of primers of the other fragments.

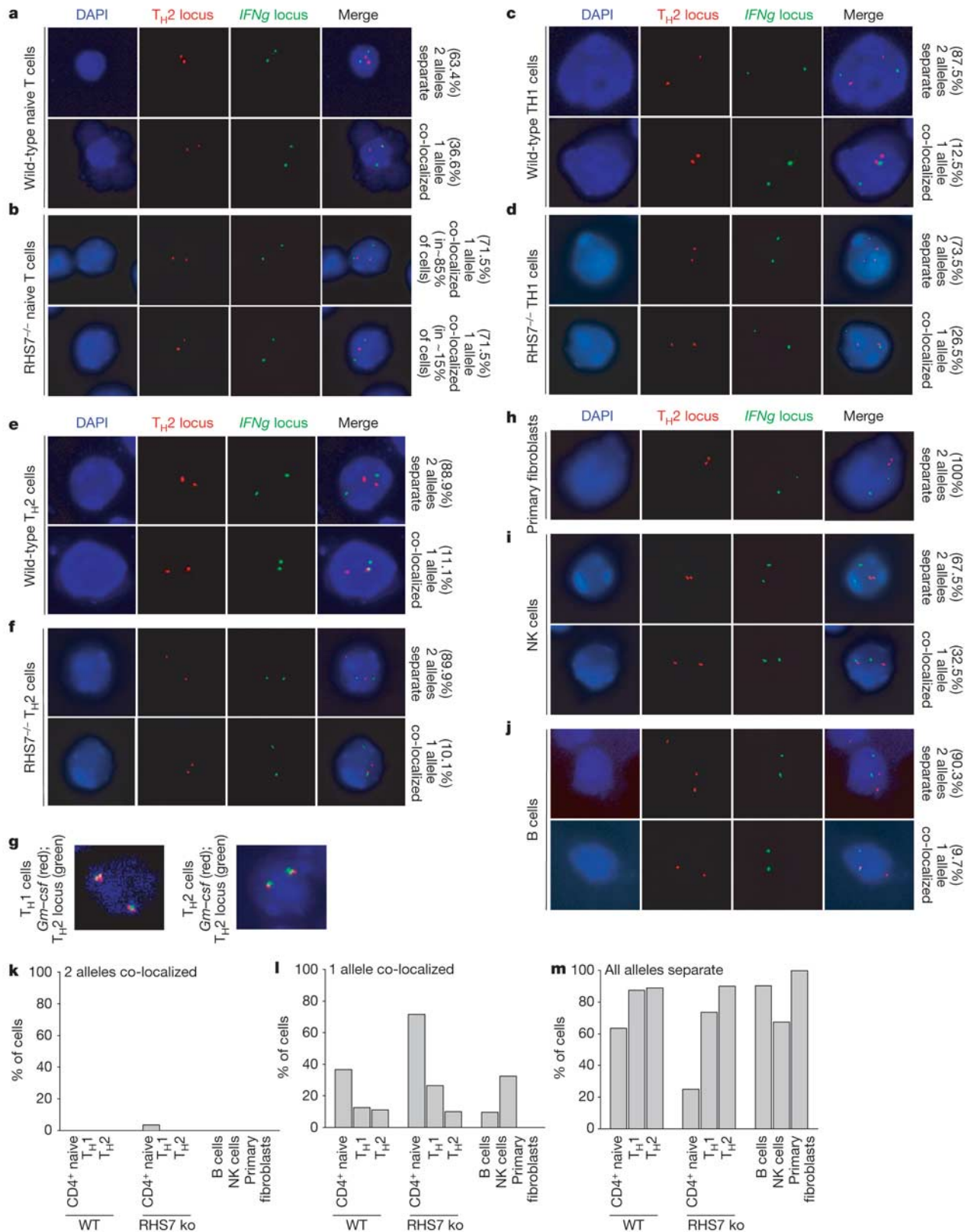


**Figure 4 | Co-localization of the *Ifng* and  $T_{H2}$  loci as revealed by FISH.** Hybridization of naive T cells (a, b),  $T_{H1}$  cells (c, d),  $T_{H2}$  cells (e, f), primary fibroblasts (h), NK cells (i) and B cells (j), with rhodamine-dUTP-labelled probe for the  $T_{H2}$  locus and SpectrumGreen-dUTP-labelled probe for the *Ifng* locus. The first column of photomicrographs ( $\times 100$ ) represents DAPI staining of the nuclei for the presence of DNA. g, Hybridization of  $T_{H1}$  and  $T_{H2}$  cells with probes for *Gm-csf* and  $T_{H2}$  loci. k-m, Diagrammatic representation of the percentage of cells with co-localization. The following number of cells were scored for each cell type: wild-type naive T cells, 235; wild-type  $T_{H1}$ , 149; wild-type  $T_{H2}$ , 125;  $RHS7^{-/-}$  naive, 133;  $RHS7^{-/-}$   $T_{H1}$ ,

84;  $RHS7^{-/-}$   $T_{H2}$ , 93; primary fibroblasts, 52; B cells, 54; NK cells, 73. Signals with a relative distance of  $\leq 5$  pixels were scored as co-localized for all cell types with the exception of  $RHS7^{-/-}$  cells, where the distance of co-localized signals was  $\leq 8$  pixels. The average diameter (in pixels) of each cell nucleus was: (presented as the mean  $\pm$  s.d.) naive cells  $126.58 \pm 34.03$ ;  $T_{H1}$   $172.46 \pm 21.75$ ;  $T_{H2}$   $146.06 \pm 31.67$ ; B cells  $139.1 \pm 18.67$ ; NK cells  $135.05 \pm 19.68$ ; primary fibroblasts  $184.23 \pm 24.7$ . All cells for each category were scored blindly and slides were prepared from two different preparations of cells.

implying that the *Ifng* and  $T_{H2}$  loci still co-localize in  $RHS7^{-/-}$  cells, but in a looser manner. As a positive control for co-localization we hybridized cells with probes for the  $T_{H2}$  locus and the *Gm-csf* gene locus, both of which are on the same chromosome about 600 kb apart. In this case all signals were co-localized (Fig. 4g). We also quantified the distance between the co-localized *Ifng* and *Il4* gene regions in an additional random sample of cells. Although these two loci were  $1.87 \pm 1.97$  pixels apart in wild-type naive T cells, the distance ( $4.45 \pm 2.37$ ) was two–three times greater in  $RHS7^{-/-}$

naive T cells. This difference was highly significant ( $P < 0.001$ ). In total, we analysed approximately 1,000 cells of wild-type and  $RHS7$  knockout mice in eight experiments. Thus, by two independent approaches (3C and FISH), interchromosomal interactions were detected between the *Ifng* and  $T_{H2}$  loci in naive T cells, and were reduced in effector T cells.

We also analysed the interaction of the *Ifng* and the  $T_{H2}$  loci for natural killer (NK) cells, B cells and primary fibroblasts (Fig. 4h–j). NK cells, which have the potential to express  $IFN-\gamma$ , also show a

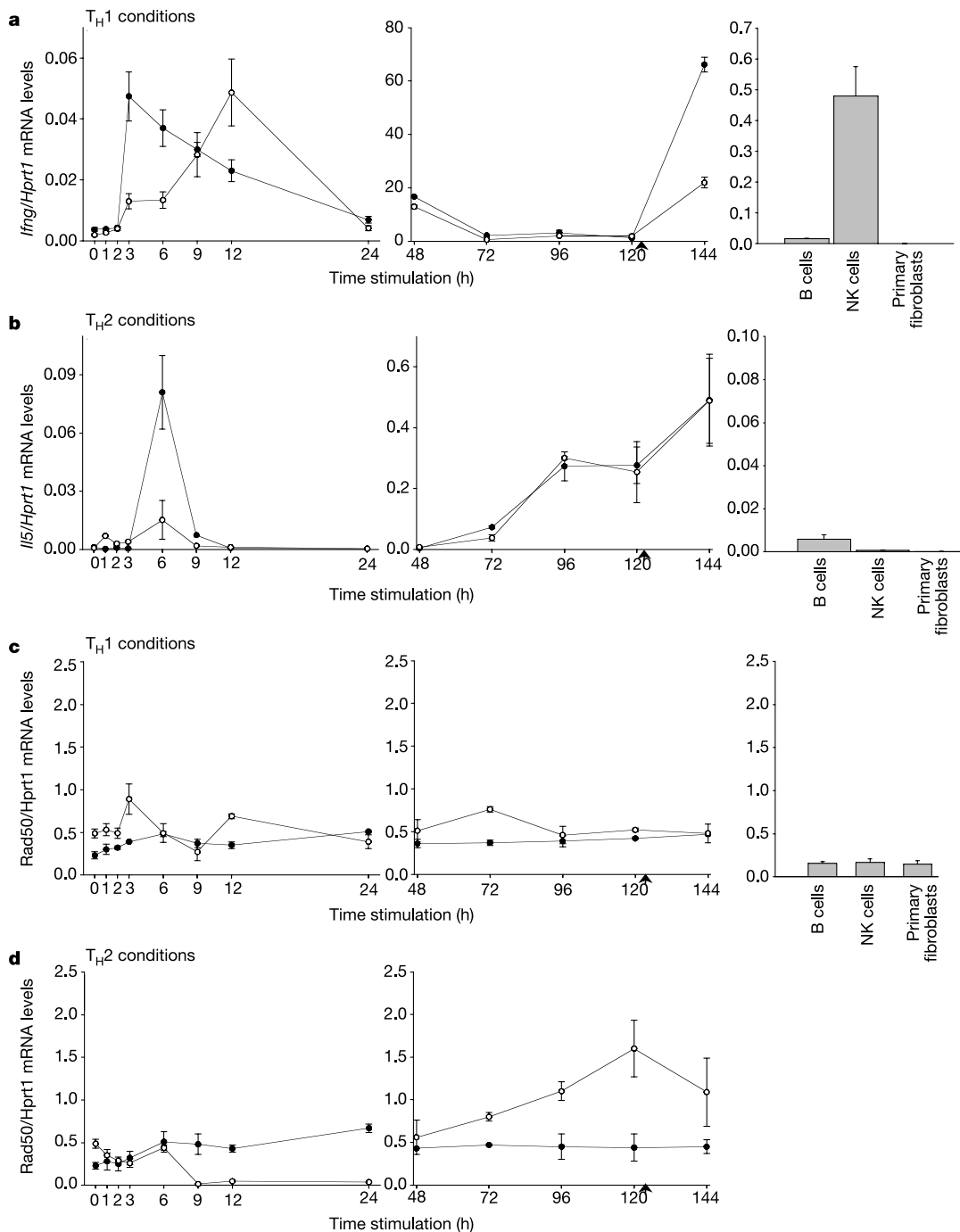


**Figure 5** | Deletion of  $RHS7$  hypersensitive site on chromosome 11 affects the expression of *Ifng* on chromosome 10. **a**, *Ifng* mRNA expression levels corrected for the expression levels of *Hprt1* ( $y$  axis) for wild-type (filled circles) and  $RHS7^{-/-}$  (open circles) sorted  $CD4^+$  naive T cells differentiated under  $T_{H1}$  conditions. The corrected *Ifng* mRNA expression levels of B cells, NK cells and primary fibroblasts are indicated on the right.

**b**, *Il5* mRNA expression levels of cells differentiated under  $T_{H2}$  conditions. **c**, **d**, *Rad50* mRNA expression levels of cells differentiated under  $T_{H1}$  (**c**) or  $T_{H2}$  (**d**) conditions. Error bars represent the standard deviation of two repeats each of three preparations of cells, with real time RT–PCR reactions performed in duplicates.

high degree of association between the *Ifng* and  $T_{H2}$  loci in 32.5% of the cells scored (Fig. 4l). Non-expressing B cells and fibroblasts, however, showed a low degree of association. A summary of the percentages of cells with co-localized or separate signals is depicted in Fig. 4k–m.

We examined whether the localization of the  $T_{H2}$  and *Ifng* loci, and especially the co-localized loci, were located in an active or an inactive nuclear compartment. We compared co-localization of the cytokine loci with DAPI (4,6-diamidino-2-phenylindole) staining for DNA (which highlights condensed heterochromatic regions), and performed immuno-DNA FISH experiments using an antibody for heterochromatin protein 1 alpha (HP1- $\alpha$ ), a protein that is mainly located in heterochromatic regions<sup>29,30</sup>. Only 7.1% of the co-localized loci in wild-type naive T cells and 8.8% of the co-localized loci in *RHS7*<sup>-/-</sup> naive T cells were located in heterochromatic regions (Supplementary Fig. 2). On the basis of this finding we propose that co-localization of the  $T_{H2}$  and the *Ifng* loci poises or prepares these loci for their rapid expression upon stimulation<sup>31–33</sup> rather than holding them in a repressive environment.

#### Interchromosomally interacting loci are poised for transcription.

Upon *in vitro* stimulation of CD4<sup>+</sup> naive T cells under  $T_{H1}$  and/or  $T_{H2}$  conditions there is an early production of cytokines, with the peak of their expression at 2–3 h after stimulation, which occurs days before the naive cells differentiate to  $T_{H1}$  or  $T_{H2}$  cells<sup>5</sup>. We sorted CD4<sup>+</sup> naive T cells from wild-type and *RHS7*<sup>-/-</sup> mice and stimulated them *in vitro* with plate-bound anti-CD3 and anti-CD28 antibodies under  $T_{H1}$  or  $T_{H2}$  conditions. At the indicated time points (Fig. 5a–d) cells were collected, and upon preparation of RNA and complementary DNA, real-time RT-PCR analysis was performed. Upon stimulation of the cells there was a rapid, transient peak of transcription at 3 h for *Ifng* production under  $T_{H1}$  conditions for the wild-type cells, whereas this peak was delayed by 9 h for the *RHS7*<sup>-/-</sup> cells. After 5 days of stimulation, by which time we obtained differentiated effector  $T_{H1}$  and  $T_{H2}$  cells, we re-stimulated the  $T_{H1}$  cells for 24 h; the production of *Ifng* was reduced threefold in the *RHS7*<sup>-/-</sup> T cells (Fig. 5a). Under the same stimulation conditions the early peak of transcription for the *Il5* gene was 6 h after stimulation under  $T_{H2}$  conditions for wild-type cells, and was decreased 5.3-fold for the *RHS7*<sup>-/-</sup> cells under the same stimulation conditions. There was no difference in production of *Il5* at late time points after stimulation for the wild-type and *RHS7*<sup>-/-</sup> cells (Fig. 5b). *Rad50* mRNA expression did not reveal any significant difference in the expression of the gene in the early compared to the late time points after stimulation (Fig. 5c,d). Thus, by several criteria, deletion of a hypersensitive site in the  $T_{H2}$  locus affects transcription of the *Ifng* locus located on a different chromosome but connected to the  $T_{H2}$  locus through an interchromosomal complex.

#### Discussion

Our study shows that there is a direct interchromosomal interaction between two loci that are expressed as mutually exclusive alternatives in two different cell types.  $T_{H1}$  cells express IFN- $\gamma$  on chromosome 10 and  $T_{H2}$  cells express IL-4, IL-5 and IL-13—the three interleukins residing as linked genes in the  $T_{H2}$  cytokine locus—on chromosome 11; these three interleukins are coordinately regulated by the action of the  $T_{H2}$  LCR and other *cis* elements. The co-localization of the *Ifng* locus with the  $T_{H2}$  locus was established with the 3C technique and confirmed with FISH experiments. The 3C interchromosomal interactions were extremely strong: they were as strong as the tightest intrachromosomal interactions that we previously described for the  $T_{H2}$  locus<sup>18</sup>.

The functional significance of the interchromosomal association is of great interest. We think that it is significant that naive CD4<sup>+</sup> T cells have the potential to rapidly express both  $T_{H1}$  and  $T_{H2}$  cytokines at low levels immediately after activation<sup>5</sup>, and we hypothesize that this is a consequence of the 'poised chromatin hub' configuration formed between the *Ifng* and  $T_{H2}$  cytokine loci, which robustly interact with

each other. The  $T_{H2}$  LCR, and more specifically the protein modules recruited to the hypersensitive sites comprising the LCR, are of great importance for this phenomenon, because the deletion of the *RHS7* site of the LCR significantly delays (9 h for *Ifng* expression) or reduces (5.3 times for the *Il5* expression) the early expression of the cytokines involved in the interchromosomal interactions. The interchromosomally interacting loci are located in a transcriptionally positive environment, and may recruit remodelling complexes or acetyltransferases to form a positive environment for the early expression of cytokines<sup>34</sup>. The fact that many nuclei of naive T cells have one co-localized pair of alleles may relate to the phenomenon of mono-allelic expression, whereby cytokines and other genes are expressed from only one of the two alleles<sup>32,35</sup>. The concept that expression might initiate first at the co-localized allele is attractive. Future RNA-FISH experiments in conjunction with DNA-FISH will help us to identify which allele is expressed first and hence determine the inter-relationships of these phenomena.

We believe that there is a dynamic interplay between partners, which is reflected by the interactions we describe. Upon differentiation of naive T cells to effector cells the interactions change: in  $T_{H1}$  cells the interchromosomal association between the *Ifng* gene and the  $T_{H2}$  cytokine locus is significantly reduced and is apparently replaced by another  $T_{H1}$ -specific interaction between the *Ifng* gene and *Ifng* CNS2, a tissue-specific transcriptional enhancer. However, we cannot be sure that this is a true 'exchange' of interactions, because with the 3C technique we detect interactions between genomic loci in a population of cells at a given time point. The structure that we describe suggests that elements located in one chromosome may positively or negatively regulate the expression of genes in a locus in another chromosome. The action of LCRs may therefore impact on not only the activation of adjacent genes but also the activation or repression of genes in other loci in the genome. Put another way, the  $T_{H2}$  LCR seems to regulate not only the transcription of the  $T_{H2}$  cytokines but also *Ifng* gene expression. On the other hand, the  $T_{H2}$  LCR may control the developmentally regulated positioning of the  $T_{H2}$  locus to the so-called transcriptional factories or other compartments of the nucleus that facilitate its expression.

The interchromosomal associations described in this work are unlikely to be restricted to T-helper cell differentiation but rather, may be a general phenomenon occurring at multiple genetic loci in the cell nucleus, particularly in gene systems where coordinate or alternative regulation is important. Potential examples include olfactory receptor genes, heavy and light chain genes of immunoglobulins, and  $\alpha$ - and  $\beta$ -globin genes, where gene expression or rearrangement might be coordinated and rendered monoallelic. Furthermore, we believe that such interactions may be important in disease. It has been proposed that position in the nucleus may control gene expression<sup>36</sup>. Proximity of two chromosomes in the same general region of the nucleus has also been suggested to contribute to rearrangements, which lead to malignancy<sup>37</sup>. For example, chronic myelogenous leukaemia (CML) is marked by the presence of a distinct cytogenetic abnormality that results from a translocation between chromosomes 9 and 22, known as the Philadelphia chromosome. Also, in murine plasmacytomas (MPCs) dysregulation of the *Myc* transcript is achieved by chromosomal translocation that juxtaposes the *c-Myc/Pvt-1* locus on chromosome 15 with one of the immunoglobulin loci on chromosomes 12 (IgH), 6 (Ig $\kappa$ ) or 16 (Ig $\lambda$ ). We propose that the developmentally regulated co-localization of multiple loci such as *Bcr* and *Abl* in the cell nucleus might result in these malignancies. Future analysis of interchromosomal interactions between candidate loci may shed light on the higher-order regulation of expression in a cell nucleus.

#### METHODS

**Mice and cell cultures.** C57BL/6 mice were derived from Jackson Laboratories. Ten to twenty spleens from 4–6-week-old C57BL/6 mice were used to make

single-cell suspensions. Isolation and differentiation of naive CD4<sup>+</sup> T cells was done as described previously<sup>38</sup>. Naive cells (1 × 10<sup>6</sup> per ml) were stimulated with plate-bound anti-CD3 (145-2C11 clone, American Type Culture Collection) and anti-CD28 mouse antibodies (Pharmingen). B cells and NK cells were isolated as described before<sup>18</sup>. Experiments performed in this study were approved by the Yale University Institutional Animal Care and Use Committee.

**3C analysis.** The protocol that was used for the 3C analysis is described elsewhere<sup>18</sup> (see also Supplementary Methods). The percentage of digestion in each different cell type was identified using real-time PCR analysis with primers spanning the *Bgl*II sites of interest (Supplementary Fig. 3). To generate control templates for the positive controls, bacterial artificial chromosome (BAC) clones were used for all the loci of interest. For the T<sub>H</sub>2 locus we used the BAC clone B182 (Genome systems), for *Ifng* locus we used the BAC clone RPCL.24-352N22 (CHORI), for *Gm-csf* we used the BAC clone RPCL.23-397C23 (CHORI), and for *Gapd* and  $\beta$ -globin loci we used PCR to amplify the regions spanning the *Bgl*II sites of interest, as described previously<sup>18</sup>. For the templates to function as positive controls for the interchromosomal 3C analysis, different BAC clones were mixed in equimolar quantities, digested and ligated. The templates were prepared two times from independent experiments and the whole set of PCR reactions was repeated at least three times. Data presented are the average of results for all PCR reactions done. An important experimental control was introduced in our analysis. All PCR signals that were considered as positive were isolated, gel extracted (Qiaquick, Qiagen), cloned in a TA vector (TA cloning kit, Invitrogen) and sequenced to identify unambiguously the sequence of the chimaeric *Bgl*II ligated fragments. The primers for the 3C analysis are available upon request.

**Two-dimensional FISH.** Sorted naive T cells, T<sub>H</sub>1 and T<sub>H</sub>2 cells were fixed in methanol:acetic acid (3:1), spotted on glass slides and air dried. Two micrograms of BAC DNA (the same BAC clones as the 3C analysis and for *Gapd* locus: RP23-216N11, CHORI) was labelled using the nick translation kit (Roche), according to the manufacturer's instructions, and either 0.05 mM rhodamine-dUTP (Roche) or 0.025 mM SpectrumGreen-dUTP (Vysis). The probe was incubated overnight (15 h) at 15 °C and then purified using the PCR purification kit (Qiagen) and eluted in 30  $\mu$ l of water. The probe mix consisted of 7  $\mu$ l master mix (60% formamide, 2 × SSC, 30% dextran sulphate), 1  $\mu$ l mouse cot-1 DNA (Roche) and 2  $\mu$ l of each probe. The signals were detected using an Olympus BX51 microscope equipped with Vysis filters. The data presented in Supplementary Fig. 1 have been generated using this protocol.

**Three-dimensional FISH.** Cells were prepared on coverslips with the following protocol, which permits the maintenance of the three-dimensional structure of the cells. Cells were permitted to attach onto poly-L-lysine-coated coverslips (BD BioCoat Cellware poly-L-lysine, 12 mm; BD Biosciences) and were fixed with 4% PFA in 0.3 × PBS for 12 min, washed three times with 1 × PBS (5 min per wash) and permeabilized with 0.5% Triton X-100 in PBS for 10 min. After an incubation of 30 min in 20% glycerol/PBS, cells were freeze-thawed three times in liquid nitrogen. Cells were incubated in 0.1N HCl for 5 min and rinsed in 2 × SSC. After the fixation and pre-treatment, the cells were stored in 50% formamide/2 × SSC. The same probes that were used for the two-dimensional FISH were also used for three-dimensional FISH in an overnight incubation. After washing the coverslips we proceeded with the immuno-FISH. An anti-HP1- $\alpha$  monoclonal antibody (MAB3584, Chemicon International) was used in a dilution of 1/400. The secondary capture antibody (A-11068, Alexa Fluor 350 goat anti-mouse, Molecular Probes) was used in a dilution of 1/200. Coverslips were mounted in VectaShield (Vector Laboratories) and were visualized using an automated Olympus BX61 microscope. All the data presented in Figs 1–5 as well as Supplementary Fig. 2 have been generated with the protocol described here.

**Real-time PCR analysis.** Quantitative reverse transcriptase (RT)-PCR was performed using real-time fluorogenic 5'-nuclease PCR using an i-cycler (Biorad) according to the manufacturer's instructions. The primers and probes used for the amplification of *Ifng*, *Il5* and *Hprt1* are described elsewhere<sup>3</sup>. The primers and probe for the amplification of *Rad50* cDNA was Mm00485504\_m1 (Applied Biosystems). Cytokine transcripts were normalized to *Hprt1* abundance. For the analysis of the percentage of the restriction enzyme digestion of templates with *Bgl*II (Supplementary Fig. 3 online) we used iQ Sybr Green Supermix (Biorad) and pairs of primers spanning the *Bgl*II sites and amplifying products of a size of 80–160 base pairs (bp). The sequences of primers are available upon request.

Received 11 February; accepted 30 March 2005.

Published online 8 May 2005.

- Cremer, T. & Cremer, C. Chromosome territories, nuclear architecture and gene regulation in mammalian cells. *Nature Rev. Genet.* **2**, 292–301 (2001).
- Spector, D. L. The dynamics of chromosome organization and gene regulation. *Annu. Rev. Biochem.* **72**, 573–608 (2003).
- Brown, K. E. *et al.* Association of transcriptionally silent genes with Ikaros complexes at centromeric heterochromatin. *Cell* **91**, 845–854 (1997).
- Brown, K. E., Baxter, J., Graf, D., Merkenschlager, M. & Fisher, A. G. Dynamic repositioning of genes in the nucleus of lymphocytes preparing for cell division. *Mol. Cell* **3**, 207–217 (1999).
- Grogan, J. L. *et al.* Early transcription and silencing of cytokine genes underlie polarization of T helper cell subsets. *Immunity* **14**, 205–215 (2001).
- Ragoczy, T., Telling, A., Sawado, T., Groudine, M. & Koxak, S. T. A genetic analysis of chromosome territory looping: diverse roles for distal regulatory elements. *Chromosome Res.* **11**, 513–525 (2003).
- Francastel, C., Walters, M. C., Groudine, M. & Martin, D. I. A functional enhancer suppresses silencing of a transgene and prevents its localization close to centromeric heterochromatin. *Cell* **99**, 259–269 (1999).
- Schubeler, D. *et al.* Nuclear localization and histone acetylation: a pathway for chromatin opening and transcriptional activation of the human  $\beta$ -globin locus. *Genes Dev.* **14**, 940–950 (2000).
- Gerasimova, T. I., Byrd, K. & Corces, V. A chromatin insulator determines the nuclear localization of DNA. *Mol. Cell* **6**, 1025–1035 (2000).
- Cobb, B. S. *et al.* Targeting Ikaros to pericentromeric heterochromatin by direct DNA binding. *Genes Dev.* **14**, 2146–2160 (2000).
- Carmo-Fonseca, M., Platani, M. & Swedlow, J. R. Macromolecular mobility inside the cell nucleus. *Trends Cell Biol.* **12**, 491–495 (2002).
- Carmo-Fonseca, M. The contribution of nuclear compartmentalization to gene regulation. *Cell* **108**, 513–521 (2002).
- Jenuwein, T. & Allis, C. D. Translating the histone code. *Science* **293**, 1074–1080 (2001).
- Mahy, N. L., Perry, P. E., Goilchrist, S., Baldock, R. A. & Bickmore, W. A. Spatial organization of active and inactive genes and noncoding DNA within chromosome territories. *J. Cell Biol.* **157**, 579–589 (2004).
- Dekker, J., Rippe, K., Dekker, M. & Kleckner, N. Capturing chromosome conformation. *Science* **295**, 1306–1311 (2002).
- Tolhuis, B., Palstra, R.-J., Splinter, E., Grosveld, F. & de Laat, W. Looping and interaction between hypersensitive sites in the active  $\beta$ -globin locus. *Mol. Cell* **10**, 1453–1465 (2002).
- Palstra, R.-J. *et al.* The  $\beta$ -globin nuclear compartment in development and erythroid differentiation. *Nature Genet.* **35**, 190–194 (2003).
- Spilianakis, C. & Flavell, R. A. Long-range intrachromosomal interactions in the T helper type 2 cytokine locus. *Nature Immunol.* **5**, 1017–1027 (2004).
- Takemoto, N. *et al.* TH2-specific DNase I-hypersensitive sites in the murine IL-13 and IL-4 intergenic region. *Int. Immunol.* **10**, 1981–1985 (1998).
- Agarwal, S. & Rao, A. Modulation of chromatin structure regulates cytokine gene expression during T cell differentiation. *Immunity* **9**, 765–775 (1998).
- Loots, G. G. *et al.* Identification of a coordinate regulator of interleukins-4, 13 and 5 by cross-species sequence comparisons. *Science* **288**, 136–140 (2000).
- Agarwal, S., Avni, O. & Rao, A. Cell-type-restricted binding of the transcription factor NFAT to a distal IL-4 enhancer *in vivo*. *Immunity* **12**, 643–652 (2000).
- Lee, G. R., Fields, P. E., Griffin, T. J. IV & Flavell, R. A. Regulation of the Th2 cytokine locus by a Locus Control Region. *Immunity* **19**, 145–153 (2003).
- Fields, P. E., Lee, G. R., Kim, S. T., Bartsevich, V. & Flavell, R. A. Th2-specific chromatin remodeling and enhancer activity in the Th2 cytokine locus control region. *Immunity* **21**, 865–876 (2004).
- Lee, D. U., Avni, O., Chen, L. & Rao, A. A distal enhancer in the IFN- $\gamma$  locus revealed by genome sequence comparison. *J. Biol. Chem.* **279**, 4802–4810 (2004).
- Shnyreva, M. *et al.* Evolutionarily conserved sequence elements that positively regulate IFN- $\gamma$  expression in T cells. *Proc. Natl Acad. Sci. USA* **101**, 12622–12627 (2004).
- Lee, G. R., Spilianakis, C. & Flavell, R. A. Hypersensitive site 7 of the TH2 locus control region is essential for expressing TH2 cytokine genes and for long-range intrachromosomal interactions. *Nature Immunol.* **6**, 42–48 (2005).
- Eivazova, E. R. & Aune, T. M. Dynamic alterations in the conformation of the *Ifng* gene region during T helper cell differentiation. *Proc. Natl Acad. Sci. USA* **101**, 251–256 (2004).
- Taddei, A., Maison, C., Roche, D. & Almouzni, G. Reversible disruption of pericentric heterochromatin and centromere function by inhibiting deacetylases. *Nature Cell Biol.* **3**, 114–120 (2001).
- Schmiedeberg, L., Weisshart, K., Diekmann, S., Meyer zu Horst, G. & Hemmerich, P. High- and low-mobility populations of HP1 in heterochromatin of mammalian cells. *Mol. Biol. Cell* **15**, 2819–2833 (2004).
- Eggenschwiler, J. *et al.* Mouse mutant embryos overexpressing IGF-II exhibit phenotypic features of the Beckwith–Wiedemann and Simpson–Golabi–Behmel syndromes. *Genes Dev.* **11**, 3128–3142 (1997).
- Dong, C. & Flavell, R. A. Cell fate decision: T-helper 1 and 2 subsets in immune responses. *Arthritis Res.* **2**, 179–188 (2000).
- Guo, L. *et al.* In TH2 cells the *Il4* gene has a series of accessibility states associated with distinctive probabilities of IL-4 production. *Proc. Natl Acad. Sci. USA* **99**, 10623–10628 (2002).
- Kosak, S. T. & Groudine, M. Form follows function: the genomic organization of

- cellular differentiation. *Genes Dev.* **18**, 1371–1384 (2004).
35. Guo, L. *et al.* In TH2 cells the IL-4 gene has a series of accessibility states associated with distinctive probabilities of IL-4 production. *Proc. Natl Acad. Sci. USA* **99**, 10623–10628 (2002).
  36. Parada, L. A., Sotiriou, S. & Misteli, T. Spatial genome organization. *Exp. Cell Res.* **296**, 64–70 (2004).
  37. Roix, J. J., McQueen, P. G., Munson, P. J., Parada, L. A. & Misteli, T. Spatial proximity of translocation-prone gene loci in human lymphomas. *Nature Genet.* **34**, 287–291 (2003).
  38. Avni, O. *et al.* TH cell differentiation is accompanied by dynamic changes in histone acetylation of cytokine genes. *Nature Immunol.* **3**, 643–651 (2002).

**Supplementary Information** is linked to the online version of the paper at [www.nature.com/nature](http://www.nature.com/nature).

**Acknowledgements** We thank Wyeth Laboratories for donation of IL-12. We

also thank F. Manzo for assistance with manuscript preparation, T. Gerasimova for suggestions with the FISH protocols, and D. Sakkas for use of his fluorescence microscope. We are also grateful to F. G. Grosveld and W. de Laat for originally providing us with detailed protocols and help with establishing the 3C technique. We would like to thank C. Szekeley for assistance with graphs. C.S. is supported by a Cancer Research Institute fellowship; M.D.L. is partly supported by a Human Frontiers Science Program long-term fellowship; T.T. is supported by a Ruth L. Kirchstein NIH/NRSA/NIA post-doctoral fellowship; R.A.F. is an Investigator of the Howard Hughes Medical Institute.

**Author Information** Reprints and permissions information is available at [npg.nature.com/reprintsandpermissions](http://npg.nature.com/reprintsandpermissions). The authors declare no competing financial interests. Correspondence and requests for materials should be addressed to R.A.F. ([richard.flavell@yale.edu](mailto:richard.flavell@yale.edu)).